



## Research Article

<https://doi.org/10.1631/jzus.B2100988>



# *Spirulina platensis* aqueous extracts ameliorate colonic mucosal damage and modulate gut microbiota disorder in mice with ulcerative colitis by inhibiting inflammation and oxidative stress

Jian WANG<sup>1\*</sup>, Liqian SU<sup>1,2\*</sup>, Lun ZHANG<sup>1</sup>, Jiali ZENG<sup>1</sup>, Qingru CHEN<sup>1</sup>, Rui DENG<sup>1</sup>, Ziyang WANG<sup>1</sup>, Weidong KUANG<sup>1</sup>, Xiaobao JIN<sup>1</sup>, Shuiqing GUI<sup>3</sup>, Yinghua XU<sup>4</sup>✉, Xuemei LU<sup>1</sup>✉

<sup>1</sup>Guangdong Provincial Key Laboratory of Pharmaceutical Bioactive Substances, School of Life Science and Biopharmaceutics, Guangdong Pharmaceutical University, Guangzhou 510006, China

<sup>2</sup>School of Pharmacy, Guangdong Pharmaceutical University, Guangzhou 510006, China

<sup>3</sup>Intensive Care Unit, Shenzhen Second People's Hospital, the First Affiliated Hospital of Shenzhen University, Shenzhen 518031, China

<sup>4</sup>Key Laboratory of the Ministry of Health for Research on Quality and Standardization of Biotech Products, National Institutes for Food and Drug Control, Beijing 102629, China

**Abstract:** Ulcerative colitis (UC) is a chronic and recurrent inflammatory bowel disease (IBD) that has become a major gastroenterologic problem during recent decades. Numerous complicating factors are involved in UC development such as oxidative stress, inflammation, and microbiota disorder. These factors exacerbate damage to the intestinal mucosal barrier. *Spirulina platensis* is a commercial alga with various biological activity that is widely used as a functional ingredient in food and beverage products. However, there have been few studies on the treatment of UC using *S. platensis* aqueous extracts (SP), and the underlying mechanism of action of SP against UC has not yet been elucidated. Herein, we aimed to investigate the modulatory effect of SP on microbiota disorders in UC mice and clarify the underlying mechanisms by which SP alleviates damage to the intestinal mucosal barrier. Dextran sulfate sodium (DSS) was used to establish a normal human colonic epithelial cell (NCM460) injury model and UC animal model. The mitochondrial membrane potential assay 3-(4,5-dimethylthiazol-2-yl)-2,5-diphenyltetrazolium bromide (MTT) and staining with Annexin V-fluorescein isothiocyanate (FITC)/propidium iodide (PI) and Hoechst 33258 were carried out to determine the effects of SP on the NCM460 cell injury model. Moreover, hematoxylin and eosin (H&E) staining, transmission electron microscopy (TEM), enzyme-linked immunosorbent assay (ELISA), quantitative real-time polymerase chain reaction (qPCR), western blot, and 16S ribosomal DNA (rDNA) sequencing were used to explore the effects and underlying mechanisms of action of SP on UC in C57BL/6 mice. In vitro studies showed that SP alleviated DSS-induced NCM460 cell injury. SP also significantly reduced the excessive generation of intracellular reactive oxygen species (ROS) and prevented mitochondrial membrane potential reduction after DSS challenge. In vivo studies indicated that SP administration could alleviate the severity of DSS-induced colonic mucosal damage compared with the control group. Inhibition of inflammation and oxidative stress was associated with increases in the activity of antioxidant enzymes and the expression of tight junction proteins (TJs) post-SP treatment. SP improved gut microbiota disorder mainly by increasing antioxidant enzyme activity and the expression of TJs in the colon. Our findings demonstrate that the protective effect of SP against UC is based on its inhibition of pro-inflammatory cytokine overproduction, inhibition of DSS-induced ROS production, and enhanced expression of antioxidant enzymes and TJs in the colonic mucosal barrier.

**Key words:** *Spirulina platensis* aqueous extracts; Ulcerative colitis; Oxidative stress; Inflammation; Antioxidant; Gut microbiota

## 1 Introduction

Ulcerative colitis (UC) is a chronic and relapsing inflammatory bowel disease (IBD) without any safe and effective treatments, and has been identified as one of the major gastroenteritis diseases in the world. The clinical symptoms of UC include bloody mucopurulent stools, bloody diarrhea, and abdominal pain. These

✉ Xuemei LU, luxuemei@gdpu.edu.cn

Yinghua XU, xuyh@nifdc.org.cn

\* The two authors contributed equally to this work

✉ Xuemei LU, <https://orcid.org/0000-0002-0571-1472>

Yinghua XU, <https://orcid.org/0000-0003-2245-3249>

Received Dec. 1, 2021; Revision accepted Feb. 16, 2022;  
Crosschecked May 5, 2022

© Zhejiang University Press 2022

symptoms are associated with intestinal disorders and mucosal damage to the colon and rectum (Kaplan, 2015). The exact pathogenesis of UC remains unclear and controversial. However, emerging scientific research evidence supports the hypothesis that the etiology of UC may be related to an involute interaction among genetic susceptibility, micro-environmental factors, defective innate and acquired immune responses, colorectal epithelial barrier dysfunction, and dysregulation of gut microbiota (Cani et al., 2009; Sun et al., 2020b; Luo and Luo, 2021). The intestinal mucosal barrier, inflammation, oxidative stress, and gut microbes play critical roles in the occurrence and development of UC (Wargo, 2020). The mucosal barrier comprises mainly tight junction proteins (TJs) and intestinal epithelial cells, and serves as the first barrier for defense against a hostile external environment (Li et al., 2020). TJs are intercellular adhesion complexes composed of accessory proteins (zonula occludens) and transmembrane proteins (occludins and claudins), which have been reported to inhibit the invasion of harmful microbes and prevent pathogens crossing the epithelial membrane (Berruien and Smith, 2020; Ye et al., 2020). In addition, TJ-associated integral membrane proteins are thought to be essential for maintaining intestinal epithelial integrity by binding to the actin cytoskeleton. Perturbation of the normal gut microbial balance can disrupt the function of the intestinal barrier, allowing toxins, luminal bacteria, and antigens into the body, leading to continuous intestinal mucosal inflammation and excessive oxidative stress (Betanzos et al., 2013; Akimoto et al., 2016). Although a basal level of oxidative stress is important for normal cell function, excessive oxidative stress may exacerbate intestinal barrier impairment and epithelial cell death (Kruidenier et al., 2003). Coordination of mucosal immune cells and the intestinal epithelial network can strengthen barrier function, prevent mucosal infections, and maintain a healthy microbiota (Halfvarson et al., 2017). Considering the significant roles of these factors in UC, more attention should be paid to maintaining the intestinal mucosal barrier function. In addition, the dynamic balance of the intestinal microbiota should be considered when seeking alternative UC therapeutic strategies.

A fiber-rich diet impacts the human microbiome by influencing the broad classes of metabolites that may modify health (Liu et al., 2020). A high dietary

fiber intake is related to a lower incidence of IBDs (Emamie et al., 2021). *Spirulina platensis*, a blue-green microalga, is a popular dietary supplement owing to its rich nutritional and medicinal value and the functional diversity of its pharmacologically active components, such as soluble dietary fiber, polyunsaturated fatty acids, proteins, vitamins, polysaccharides, and essential amino acids (Kose et al., 2017; Alwaleed et al., 2021). Commercial aqueous algal extracts display activity such as anti-inflammatory, antioxidant, and anti-bacterial activity, virus resistance, immunity regulation, and hyperlipidemia reduction (Park et al., 2018). However, little is known about the effects mediated by *S. platensis* aqueous extracts (SP) in a dextran sulfate sodium (DSS)-induced colitis mouse model, such as colonic mucosal barrier function protection and especially gut microbiota modulation, and in an NCM460 injury model caused by DSS. Moreover, the potential modulatory mechanisms of SP in UC have not been verified. The objective of this study was to explore the potential protective effects of SP against DSS-induced colitis and elucidate the underlying mechanisms.

## 2 Materials and methods

### 2.1 Materials

DSS (36–50 kDa) was obtained from MP Bio-medicals (Santa Ana, CA, USA). Dimethyl sulfoxide (DMSO) was obtained from Aladdin (Shanghai, China). 3-(4,5-Dimethylthiazol-2-yl)-2,5-diphenyltetrazolium bromide (MTT), Annexin V-fluorescein isothiocyanate (FITC), propidium iodide (PI), JC-1 probe, and 2,7-dichlorodihydro fluorescein diacetate (DCFH-DA) probe were supplied by Beyotime Biotechnology Co., Ltd. (Shanghai, China). Sulfasalazine (SASP) enteric-coated tablets were purchased from the Shanghai Forward Pharmaceutical Co., Ltd. (Shanghai, China). Dulbecco's modified Eagle's medium (DMEM) and fetal bovine serum (FBS) were purchased from Gibco (Grand Island, NY, USA). Superoxide dismutase (SOD), malondialdehyde (MDA), catalase (CAT), myeloperoxidase (MPO), and glutathione peroxidase (GSH-Px) detection kits were purchased from the Nanjing Jiancheng Bioengineering Institute (Nanjing, China). Enzyme-linked immunosorbent assay (ELISA) kits were acquired from Andy Gene Biotechnology

Co., Ltd. (Beijing, China). All other chemicals used were of analytical reagent grade and were commercially available.

## 2.2 Preparation of SP

Pure food-grade *S. platensis* powder was purchased from the Gansu Yalan Pharmaceutical Co., Ltd. (Gansu, China). SP was prepared according to the following procedure. First, food-grade *S. platensis* powder was extracted with distilled water (1:10, mass/volume) at 40 °C for 7 h under magnetic stirring. Then, the reaction solution was centrifuged at 10 000 r/min for 10 min and the supernatant was lyophilized as SP. The SP sample was stored in an air-tight brown bottle at -20 °C.

## 2.3 Cell culture and DSS-induced NCM460 cells injury model

A normal human colonic epithelial cell line (NCM460) was cultured in DMEM supplemented with 1% (volume fraction) penicillin/streptomycin (Invitrogen, Carlsbad, CA, USA) and 10% (volume fraction) FBS. All cultures were incubated in a humidified atmosphere of 95% air and 5% CO<sub>2</sub> at 37 °C. The DSS-induced NCM460 cells injury model was established (Xu et al., 2018). First, the cells were plated and grown to 80% confluence prior to treatment with drugs. After 12 h, the cells were exposed to DSS at 10 mg/mL for an additional 12 h.

## 2.4 MTT assay

MTT assays were performed to investigate the effect of different concentrations of SP (50 and 100 µg/mL) on DSS-induced NCM460 cell injury. When NCM460 cells were grown to 80% confluence, they were treated with SP. After incubation for 12 h, the cells were incubated with 10 mg/mL DSS for another 12 h. Subsequently, the medium was discarded, and 20 µL MTT (5 mg/mL) solution was added to each well and incubated with the NCM460 cells for an additional 4 h. After removing the MTT medium, 100 µL of DMSO solution was added to each well, and the mixture was then shaken for 10 min in the dark to dissolve the formazan crystals. A microplate reader (BioTek SynergyH1, Winooski, VT, USA) was used to measure absorbance at 570 nm (Ciapetti et al., 1993). Each experiment was performed independently three times.

## 2.5 Apoptosis detection using Annexin V-FITC/PI

Apoptosis was detected using flow cytometry with the Annexin V-FITC/PI Apoptosis Detection Kit (Beyotime Biotechnology, Shanghai, China). NCM460 cells were digested with trypsin without ethylenediamine tetraacetic acid (EDTA), and collected in tubes. The cells were centrifuged at 1000 r/min for 3 min and washed with ice-cold phosphate-buffered saline (PBS). After that, the NCM460 cells were resuspended in 195 µL of binding buffer (1×) and stained with 5 µL of Annexin V-FITC and 10 µL of PI for 15 min without light (Eray et al., 2001). Finally, the rates of apoptosis of the prepared samples were measured using a CytoFLEX flow cytometer (Beckman Coulter, Miami, FL, USA).

## 2.6 Hoechst 33258 staining

Hoechst 33258 staining was performed according to the protocol of the Hoechst Staining Kit (Beyotime Biotechnology, Shanghai, China). NCM460 cells were stained with Hoechst 33258 staining solution for 20 min in the dark and then washed three times with PBS. The nuclear morphology of the cells was observed under a fluorescence microscope (Zeiss, Oberkochen, Germany).

## 2.7 Intracellular reactive oxygen species detection

The levels of intracellular reactive oxygen species (ROS) were assessed using a ROS assay kit (Beyotime Biotechnology, Shanghai, China). In brief, the cells were incubated with DCFH-DA solution (10 µmol/L) at 37 °C for 30 min in the dark and then washed three times with serum-free DMEM. Finally, a CytoFLEX flow cytometer was used to measure the fluorescence intensity of ROS in each group within 30 min (Prasad et al., 2019).

## 2.8 Mitochondrial membrane potential detection

Changes in the mitochondrial membrane potential (MMP,  $\Delta\Psi_m$ ) of NCM460 cells were evaluated using an MMP assay kit with a JC-1 probe (Beyotime Biotechnology, Shanghai, China). The NCM460 cells were stained with JC-1 staining solution (5 µmol/L) for 20 min at 37 °C in the dark. A fluorescence microscope (Zeiss, Oberkochen, Germany) was used to monitor the MMP by determining the relative amounts of dual emissions from mitochondrial JC-1 aggregates

(excitation at 585 nm and emission at 590 nm) or monomers (excitation at 514 nm and emission at 529 nm) (Reers et al., 1995).

## 2.9 Animals and colitis model establishment

Six-week-old SPF C57BL/6 mice were obtained from the Center for Experimental Animals, Guangdong Province (Guangzhou, China; approval No. SCXK (Yue) 2013-0002). All animals were housed in cages and had free access to food and drinking water (room temperature (23±2) °C and (55±10)% relative humidity) with a 12 h/12 h light/dark cycle for one week before commencement of the animal experiment. The animal experimental protocols and use of animals complied with the Guidelines for the Care and Use of Experimental Animals, Guangdong Pharmaceutical University (approval No. SYXK (Yue) 2012-0125) and were approved by the Guangdong Pharmaceutical University Animal Care and Use Committee, China. The acute UC model was induced by means of free drinking of sterilized water containing 2.5% (25 mg/mL) DSS for 8 d (Eichele and Kharbanda, 2017). Simultaneously, the mice with UC were orally administered 0.5% (volume fraction) sodium carboxymethylcellulose (CMC-Na). A total of 40 mice were randomly divided into four groups, as follows: normal group (Normal; drinking water and 0.5% CMC-Na), DSS-induced colitis group (Control; 2.5% DSS and 0.5% CMC-Na), SP treatment group (SP; 2.5% DSS with intragastric (i.g.) administration of 300 mg/kg SP), and SASP treatment group (SASP; 2.5% DSS, with i.g. administration of 300 mg/kg SASP). Changes in the physiological state and body weights of the mice were recorded in detail throughout the period (11 d), to evaluate the disease activity index (DAI). The DAI was calculated by scoring the average body weight, gross bleeding, and stool consistency (severity was graded from 0 to 4 for each index) (Sokol and Beaugerie, 2010). Blood was centrifuged to obtain the serum to be preserved at -80 °C. The colon tissues were immediately excised and photographed. A small segment of the colon tissue was removed for histological assessment. The remaining colon tissues were snap-frozen in liquid nitrogen and stored for subsequent biochemical assays.

## 2.10 Hematoxylin and eosin staining

Colon tissues were rapidly excised, placed in 4% (volume fraction) paraformaldehyde, and embedded

in paraffin. Next, the tissues were cut into 5- $\mu$ m-thick sections using a RM2235 microtome (Leica, Solms, Germany) and adhered to glass slides for hematoxylin and eosin (H&E) staining. Histopathological scores of the colons were evaluated in a blinded fashion by three different investigators, using criteria described previously (Takagi et al., 2011). A light microscope with a digital camera (Zeiss, Oberkochen, Germany) was used to capture the images.

## 2.11 Transmission electron microscopy

In this study, transmission electron microscopy (TEM) was used to observe changes in the colon ultrastructure in each group. Briefly, colon tissues were sliced into cubic millimeters and rapidly fixed in 2.5% (volume fraction) glutaraldehyde for 12 h at -4 °C. After washing the samples three times in PBS, they were fixed in 1% (volume fraction) osmium tetroxide for 2 h. Subsequently, after dehydration in an ethanol gradient and embedding in epoxy resin, the tissue was treated with 2% (volume fraction) uranyl acetate for 1 h. Finally, a JEM1400 transmission electron microscope (Jeol, Tokyo, Japan) was used to observe and photograph the samples. The damage to the colonic microstructure in each group was scored according to the scoring standard used in a previous study (Zhang et al., 2021).

## 2.12 ELISA

To evaluate the effects of SP on inflammatory and immunological responses in UC mice, the levels of tumor necrosis factor- $\alpha$  (TNF- $\alpha$ ), interferon- $\gamma$  (IFN- $\gamma$ ), interleukin-6 (IL-6), IL-1 $\beta$ , IL-17, IL-10, and diamine oxidase (DAO) in serum and colon tissues were measured using commercially available ELISA kits. All calculation methods and detection steps were performed according to the ELISA kit protocol.

## 2.13 Measurements of MPO, SOD, CAT, and GSH-Px activity and MDA content assays

Colon tissues were homogenized in cold saline to prepare the colon supernatants. MPO, SOD, CAT, and GSH-Px activity, and MDA content were determined using kits. All experimental operations and data processing were performed according to the manufacturer's protocol.

## 2.14 Quantification of gene expression

Samples from the distal colons were washed three times with PBS, and then stored in RNA save solution (TaKaRa Biotechnology Co., Ltd., Kusatsu, Japan) until they were used for total RNA extraction. Total RNA extraction and complementary DNA (cDNA) synthesis were performed using TRIzol™ Reagent (Invitrogen, Carlsbad, CA, USA) and a PrimeScript™ RT Reagent Kit with gDNA Eraser (TaKaRa Biotechnology Co., Ltd., Kusatsu, Japan). In a CFX Connect fluorescence quantitative real-time polymerase chain reaction (qPCR) detection system (Bio-Rad, Hercules, CA, USA), the samples were performed using SYBR® Premix Ex Taq™ Kit (TaKaRa Biotechnology Co., Ltd., Kusatsu, Japan), and the messenger RNA (mRNA) levels of individual genes were detected. The 25- $\mu$ L PCR reaction volume contained 1  $\mu$ L of each primer (10  $\mu$ mol/L), 2  $\mu$ L cDNA reaction solution, 12.5  $\mu$ L SYBR® Premix Ex Taq™, and 8.5  $\mu$ L RNase/DNase-free distilled water. Dissociation data were analyzed according to the comparative threshold cycle ( $C_t$ ) method, and normalized to the endogenous reference glyceraldehyde-3-phosphate dehydrogenase (GAPDH) (Rao et al., 2013). The primer sequences used for qPCR are listed in Table 1.

**Table 1 qPCR primer sequences**

Gene	Primer sequence (5'→3')
<i>ZO-1</i>	F: CCAGCAACTTTCAGACCACC R: TTGTGTACGGCTTTGGTGTG
<i>Claudin-1</i>	F: TCGACTCCTTGCTGAATCTGA R: TCCACATCTTCTGCACCTCA
<i>Occludin</i>	F: GCTTACAGGCAGAACTAGACG R: TCTGCAGATCCCTTAACTTGC
<i>NF-<math>\kappa</math>B p65</i>	F: TCTTCTTGCTGTGCGACAAG R: GCATGGAGACTCGAACAGGA
<i>COX-2</i>	F: AGGTCATTGGTGGAGAGGTG R: CCTGCTTGAGTATGTCGCAC
<i>iNOS</i>	F: ACAGGAACCTACCAGCTCAC R: CGACCTGATGTTGCCATTGT
<i>GAPDH</i>	F: CCATCACCATCTTCCAGGAG R: CCTGCTTACCACCTTCTTG

*ZO-1*: zonula occludens-1; *NF- $\kappa$ B*: nuclear factor- $\kappa$ B; *COX-2*: cyclooxygenase-2; *iNOS*: inducible nitric oxide synthase; *GAPDH*: glyceraldehyde-3-phosphate dehydrogenase; F: forward; R: reverse.

## 2.15 Western blot analysis

The colon tissues were homogenized in radio-immunoprecipitation assay (RIPA) lysis buffer (Beyotime Biotechnology, Shanghai, China) containing

1 mmol/L phenylmethylsulfonyl fluoride (PMSF; Beyotime Biotechnology, Shanghai, China) to prepare the protein samples. The supernatant was collected after homogenization and centrifugation, and the protein concentration was determined using bicinchoninic acid (BCA) assay kits (Beyotime Biotechnology, Shanghai, China). The protein samples (20  $\mu$ g/well) were separated on a 5%–12% or 5%–8% (1%=10 mg/mL) sodium dodecyl sulfate-polyacrylamide gel electrophoresis (SDS-PAGE) gel and transferred to polyvinylidene fluoride (PVDF) membranes. Subsequently, the membranes were blocked with 5% (50 mg/mL) degreasing milk dissolved in triethanolamine-buffered saline (TBS) buffer for 1 h, and then incubated with the primary antibody (Abcam, Cambridge, UK) overnight at 4 °C. The primary antibodies used included those against claudin-1 (1:1000, volume ratio, the same below), occludin (1:1000), zonula occludens-1 (ZO-1, 1:1500), inducible nitric oxide synthase (iNOS, 1:1000), cyclooxygenase-2 (COX-2, 1:1000), and nuclear factor- $\kappa$ B (NF- $\kappa$ B) p65 (1:1000). After washing with TBS-containing Tween-20 (TBST), the membranes were incubated with horseradish peroxidase (HRP)-conjugated secondary antibody (1:1000; Beyotime Biotechnology, Shanghai, China) for 2 h at 20 °C. Next, the membranes were immersed in enhanced chemiluminescence (ECL) luminescence reagent (Beyotime Biotechnology, Shanghai, China), and the signals obtained were visualized using a Tanon-5200 standard chemiluminescence system (Shanghai Tanon Technology Co., Ltd., Shanghai, China). The densities of bands were analyzed using ImageJ software (Bethesda, MA, USA) and normalized to those of GAPDH after stripping and reprobing (Ida et al., 1996).

## 2.16 Gut microbiota analysis using 16S rDNA high-throughput sequencing

Twelve fecal samples were collected from each of the four groups according to sample collection standards, and stored at –80 °C temporarily. All samples were sent to Novogene Co., Ltd. (Beijing, China) for 16S ribosomal DNA (rDNA) high-throughput sequencing. High-fidelity PCR was applied to amplify bacterial 16S rDNA hypervariable region 4 (16S V4 region) using the primers. The 16S V4 region reveals the relationship between flora and corresponding indices, as well as the difference in species composition between

groups.  $\alpha$ -Diversity analysis included indices of observed operational taxonomic units (OTUs) and linear discriminant analysis effect size (LEfSe) (Siddiqui et al., 2011).

### 2.17 Statistical analysis

Statistical analyses of all experimental data were performed using Prism 7.0 software (GraphPad, La Jolla, CA, USA). Data are expressed as mean $\pm$ standard deviation of more than two independent experiments. Student's *t*-test (for two groups) or one-way analysis of variance (ANOVA) (for more than two groups) was used to assess the differences between groups. The results were considered statistically significant at  $P < 0.05$ .

## 3 Results

### 3.1 Chemical compounds in SP

*S. platensis* is a pure natural food, rich in various nutrients. There have been many reports on the therapeutic applications of *S. platensis* to treat health problems such as arthritis, cardiovascular diseases, and diabetes. The chemical compositions of *S. platensis* dry powder and aqueous extracts are listed in Tables 2 and 3, respectively.

### 3.2 Alleviation of the DSS-induced NCM460 cell injury by SP

The results of the MTT assay (Fig. 1) showed that about 50% of NCM460 cells died upon treatment with 10 mg/mL DSS in the control group. After addition of SP at different concentrations (50 and 100  $\mu$ g/mL) for 4 h, the DSS-induced decline in NCM460 cell viability was substantially inhibited in a concentration-dependent manner. The inhibitory effects of SP on NCM460 DSS-induced cell apoptosis were evaluated using flow cytometry (Annexin V-FITC/PI double staining) and Hoechst 33258 staining (Figs. 2 and 3). SP at a concentration of 100  $\mu$ g/mL (SP-H) conferred a stronger resistance to DSS-induced apoptosis in NCM460 cells than SP at a concentration of 50  $\mu$ g/mL (SP-L) (Fig. 2). NCM460 cells in the normal group were stained blue uniformly (Fig. 3). However, in the control group, the cell morphology was distinctly altered, and some morphological hallmarks of apoptosis, including cell fragments and condensed bright chromatin, were evident. These

**Table 2 Chemical composition of 100 g of *Spirulina platensis* powder**

Project	Component	Content
General component	Protein	60–70 g
	Lipids	6–9 g
	Carbohydrate	14–20 g
	Fiber	2–4 g
	Ash	4–8 g
	Phenols	2–8 g
Pigment	Chlorophyll	800–2000 mg
	Carotenoid	200–400 mg
	Phycocyanin	7000–8500 mg
Mineral substance	Calcium	100–400 mg
	Iron	50–100 mg
	Potassium	1000–2000 mg
	Magnesium	200–300 mg
Others	Vitamin A	100–200 mg
	Vitamin B1	1.5–4.0 mg
	Vitamin B2	3–5 mg
	Vitamin B3	0.5–0.7 mg
	Vitamin B4	0.4–0.7 mg
	Vitamin B12	0.05–0.20 mg
	Vitamin E	5–20 mg
	Vitamin PP	305 mg
	$\gamma$ -Linolenic acid	800–1300 mg
	Folic acid	0.05 mg
	Inositol	4–100 mg
Calcium pantothenate	1 mg	

**Table 3 Chemical compounds identified in *Spirulina platensis* aqueous extracts**

Compound	Content (%)
Total protein	75.80 $\pm$ 2.31
Total carbohydrate	12.50 $\pm$ 1.19
Total phenols	1.01 $\pm$ 0.02
Phycocyanin	13.90 $\pm$ 1.22
Phycoerythrin	0.92 $\pm$ 0.06
Allophycocyanin	6.34 $\pm$ 0.59

Data are expressed as mean $\pm$ standard deviation,  $n=3$ .

abnormalities were significantly reduced in the SP-L and SP-H groups. Altogether, SP alleviated NCM460 cell injury induced by DSS.

### 3.3 Inhibition of the DSS-induced excessive intracellular ROS production and MMP decrease in NCM460 cells by SP

Mitochondria, the primary sites of ROS production, play an essential role in the regulation of life and death; high concentrations of ROS can change the permeability of the mitochondrial membrane, inducing  $\text{Ca}^{2+}$  outflow and cytochrome C (Cyt-C) release, which

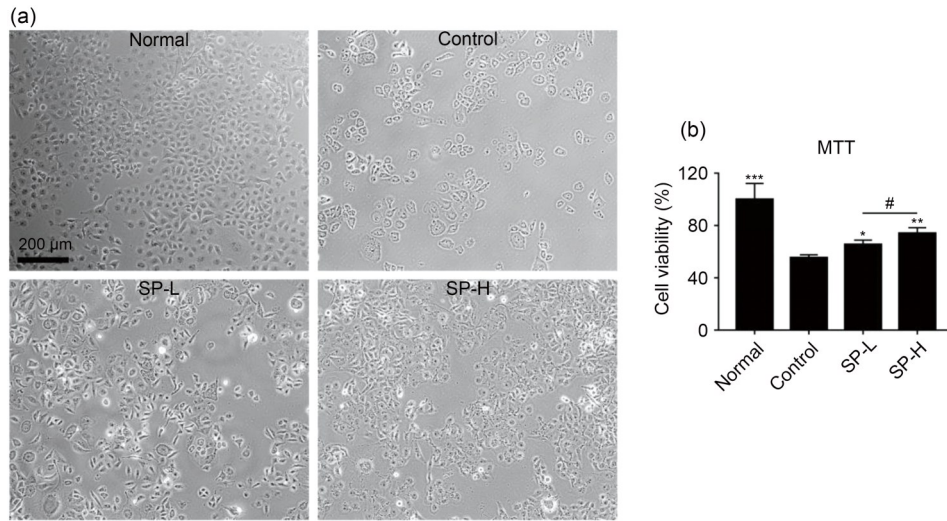


**Fig. 1** Effects of different concentrations of SP on NCM460 cell viability. (a) Representative photographs of NCM460 cells; (b) Cell viability of NCM460 cells treated with SP (0, 50, and 100 µg/mL). All data are represented as mean±standard deviation ( $n=3$ ). \*  $P<0.05$ , \*\*  $P<0.01$ , \*\*\*  $P<0.001$ , compared with the control group; #  $P<0.05$ , compared between the SP-L and SP-H groups. SP: *Spirulina platensis* aqueous extracts; SP-L: treated with 50 µg/mL SP; SP-H: treated with 100 µg/mL SP; MTT: 3-(4,5-dimethylthiazol-2-yl)-2,5-diphenyltetrazolium bromide.

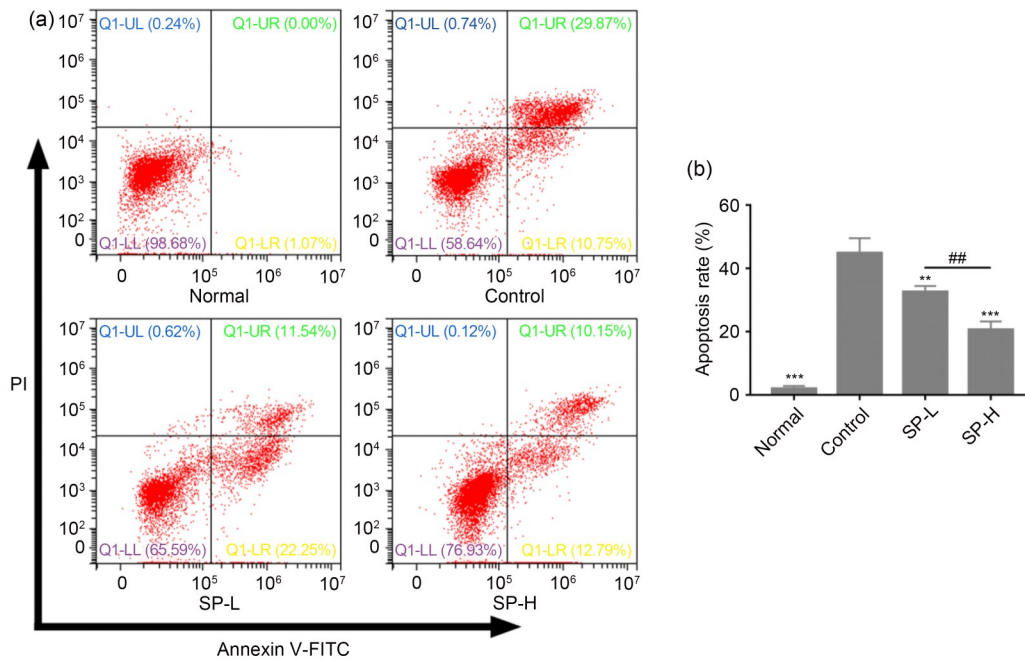


**Fig. 2** Effects of different concentrations of SP on the apoptosis rate of NCM460 cells induced by DSS. (a) The effect of SP on DSS-induced NCM460 cells apoptosis; (b) Quantitative analysis of the apoptotic cells. All values are expressed as mean±standard deviation ( $n=3$ ). \*\*  $P<0.01$ , \*\*\*  $P<0.001$ , compared with the control group; ##  $P<0.01$ , compared between the SP-L and SP-H groups. SP: *Spirulina platensis* aqueous extracts; SP-L: treated with 50 µg/mL SP; SP-H: treated with 100 µg/mL SP; DSS: dextran sulfate sodium; PI: propidium iodide; FITC: fluorescein isothiocyanate.

ultimately activates the caspase-3 pathway of apoptosis (Pardhasaradhi et al., 2003). Disruption of MMP can be used as an early indicator of cell apoptosis (Dobi et al., 2021). The effects of SP on excessive

ROS production and MMP disruption in DSS-induced NCM460 cells were evaluated. Fig. 4 shows that ROS levels decreased significantly in the SP-treated group compared with the control group. The changes

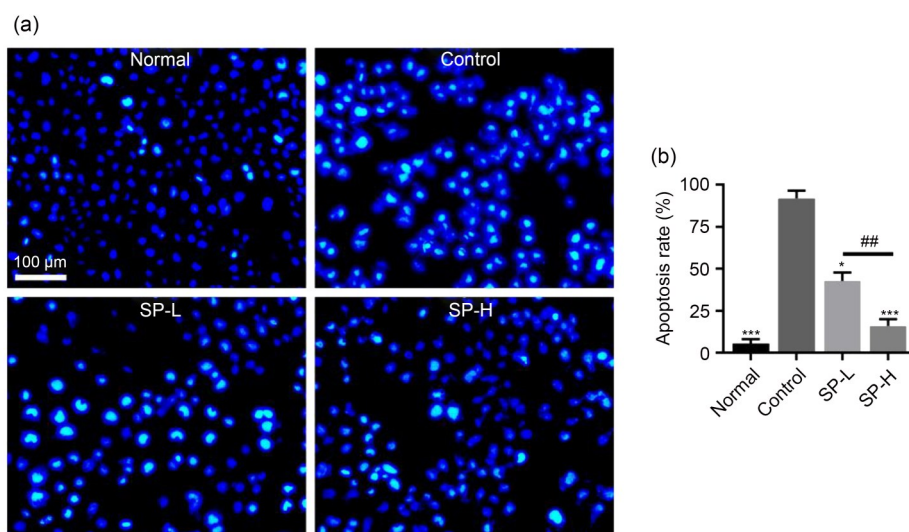


**Fig. 3** Effects of different concentrations of SP on the morphological changes of NCM460 cells induced by DSS. (a) Representative photographs of NCM460 cell morphological changes using the Hoechst 33258 fluorescence staining method. Normal nuclei are shown blue, while the nuclei of apoptotic cells appear fragmented or dense. (b) Quantitative analysis of the apoptotic rate. All values are expressed as mean±standard deviation ( $n=3$ ). \*  $P<0.05$ , \*\*\*  $P<0.001$ , compared with the control group; ##  $P<0.01$ , compared between the SP-L and SP-H groups. SP: *Spirulina platensis* aqueous extracts; SP-L: treated with 50 μg/mL SP; SP-H: treated with 100 μg/mL SP.

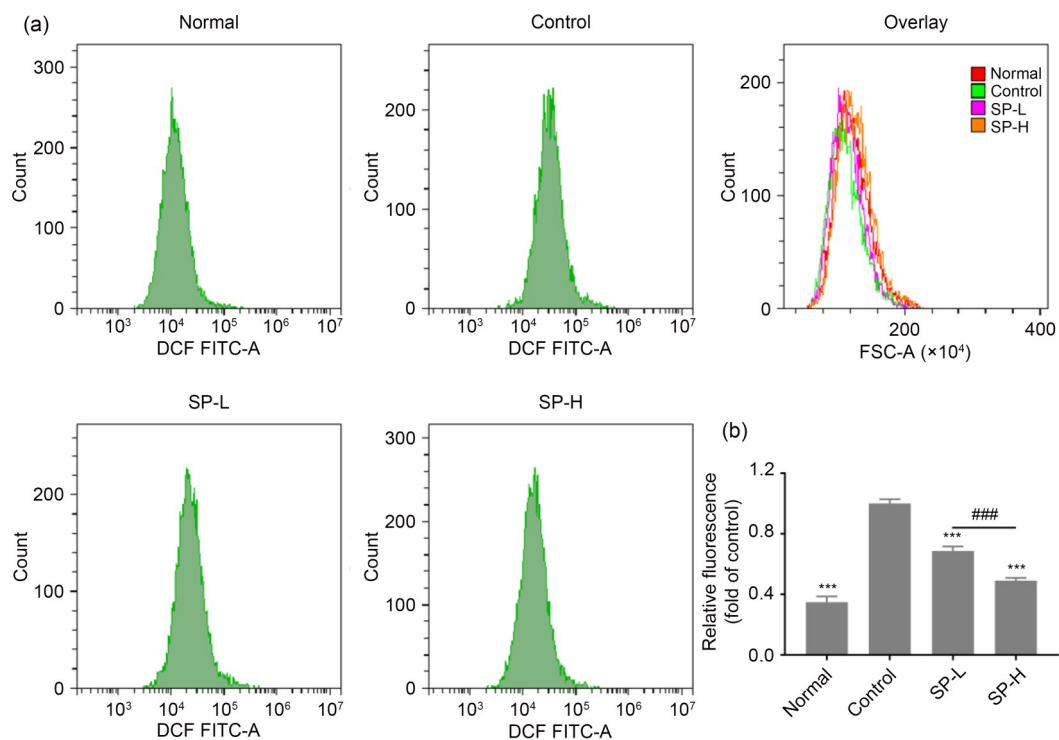


**Fig. 4** Inhibition of the DSS-induced excessive intracellular ROS production in NCM460 cells by SP. (a) The intracellular ROS levels were assessed by DCFH-DA assay. (b) The levels of ROS are presented as the corresponding statistical graph. All values are expressed as mean±standard deviation ( $n=3$ ). \*\*\*  $P<0.001$ , compared with the control group; ###  $P<0.001$ , compared between the SP-L and SP-H groups. ROS: reactive oxygen species; DCFH-DA: 2,7-dichlorodihydro fluorescein diacetate; SP: *Spirulina platensis* aqueous extracts; SP-L: treated with 50 μg/mL SP; SP-H: treated with 100 μg/mL SP; FSC-A: forward-scatter area; FITC: fluorescein isothiocyanate.

in fluorescence color reflected the changes in MMP. As shown in Fig. 5, the red fluorescence in the normal group indicated a high MMP, while the green fluorescence in the control group indicated a low MMP. There was a significant increase in MMP upon treatment with increasing concentrations of SP. These results indicated that SP could limit excessive ROS generation and MMP reduction, thereby maintaining mitochondrial function and protecting NCM460 cells from DSS-induced damage.

### 3.4 Amelioration of DSS-induced colitis in C57BL/6 mice by SP

A mouse model of colitis was successfully established by administering sterilized water containing 2.5% DSS to the animals for 8 d. SP was orally administered at a dose of 300 mg/kg to the model mice, to evaluate its potential therapeutic efficacy against colitis (Fig. 6a). Mice with DSS-induced colitis often exhibit a significant decrease in colon length, which is regarded as a morphological parameter for the degree of damage. The length of the colon in the control group was significantly shorter than that in the normal group (Fig. 6b). Additionally, in the SP group, the extent of the restriction of the shortening of the colon

was similar to that of the SASP treatment group. The body weights of mice in the control group were also significantly lower than those in the other groups (Fig. 6c). The DAI score is used to evaluate the degree of diarrhea and bloody stool during the colitis-modeling period (Tsang et al., 2019). The DAI score of the control group was higher than those of the other groups (Fig. 6d). In summary, upon SP or SASP treatment, colon shortening, weight loss, and the increase in DAI score were reduced compared with the control group, and these effects were similar between the SP and SASP groups.

In addition, the results of H&E staining and TEM (Fig. 7) confirmed that SP could ameliorate histopathological injury such as intestinal mucosal epithelial wall damage, goblet cell loss, inflammatory cell infiltration, and abnormal villus structure compared with that seen in the control group.

### 3.5 Decreased levels of inflammatory cytokines in the serum and colon upon SP treatment

Increased secretion and infiltration of inflammatory cytokines contribute greatly to the occurrence and development of colitis (Lu et al., 2019). The levels of inflammatory cytokines associated with colitis

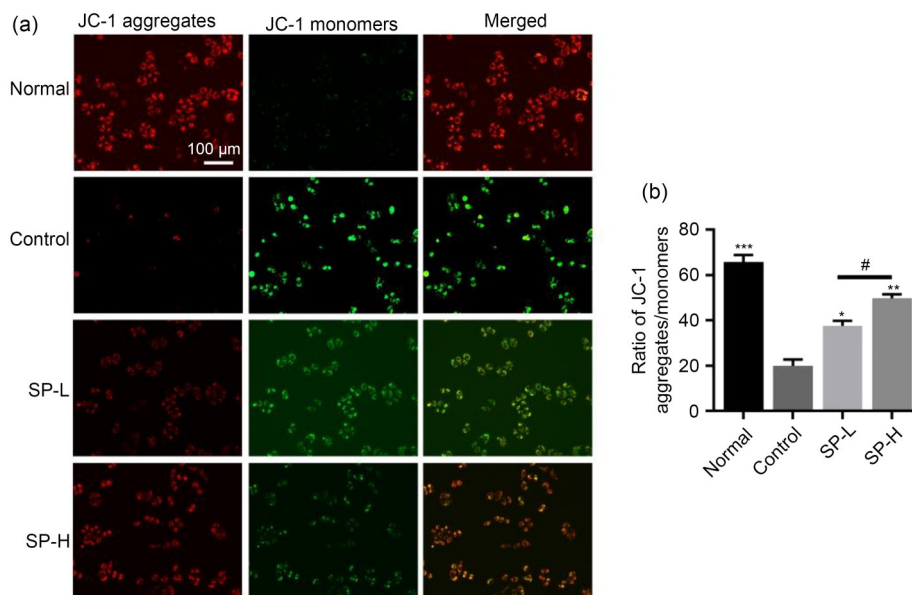


**Fig. 5** Inhibition of the DSS-induced MMP decrease in NCM460 cells by SP. (a) The MMP of cells was assessed by the JC-1 method. JC-1 aggregates with red fluorescence represent a high MMP and JC-1 monomers with green fluorescence indicate a low MMP. (b) Quantitative analysis of the ratio of JC-1 aggregates/monomers. All values are expressed as mean±standard deviation ( $n=3$ ). \*  $P<0.05$ , \*\*  $P<0.01$ , \*\*\*  $P<0.001$ , compared with the control group; #  $P<0.05$ , compared between the SP-L and SP-H groups. DSS: dextran sulfate sodium; MMP: mitochondrial membrane potential; SP: *Spirulina platensis* aqueous extracts; SP-L: treated with 50  $\mu\text{g/mL}$  SP; SP-H: treated with 100  $\mu\text{g/mL}$  SP.

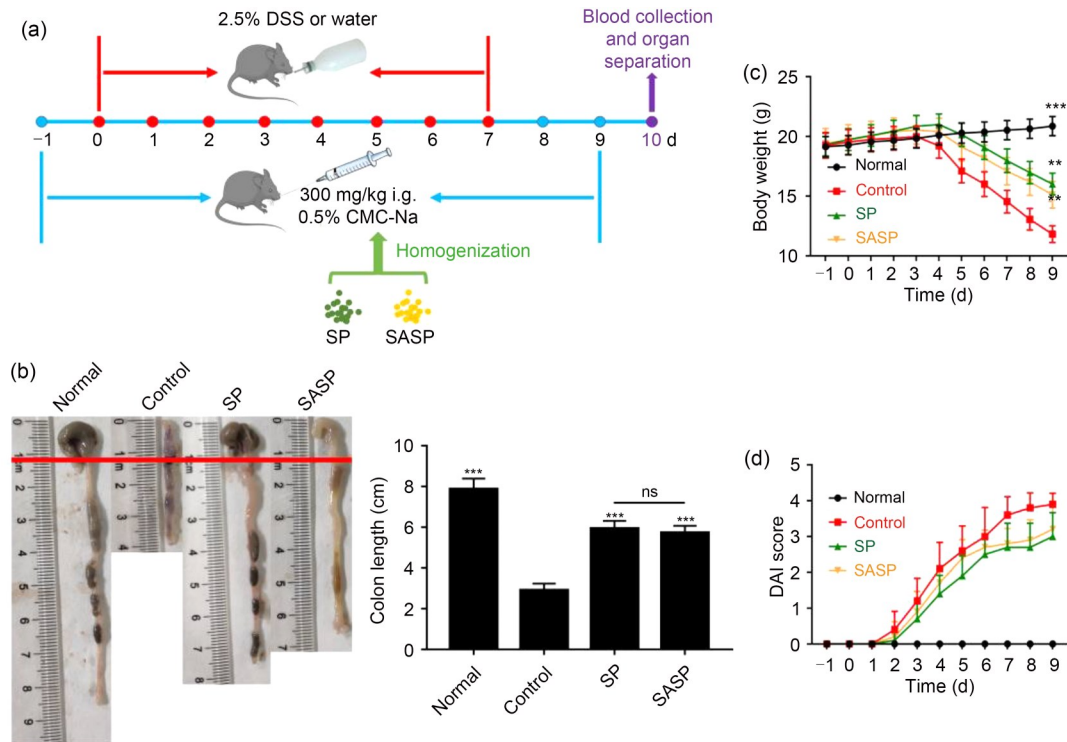


**Fig. 6** Positive effects of SP on colon length, body weight, and DAI in DSS-treated mice. (a) The animal experimental design; (b) Colon length; (c) Body weight; (d) DAI scores. Data are presented as mean±standard deviation ( $n=6$ ). \*\*  $P<0.01$ , \*\*\*  $P<0.001$ , compared with the control group; ns No significant difference between the SP and SASP groups. DAI: disease activity index; SASP: sulfasalazine; SP: *Spirulina platensis* aqueous extracts; DSS: dextran sulfate sodium; i.g.: intragastric; CMC-Na: sodium carboxymethylcellulose.

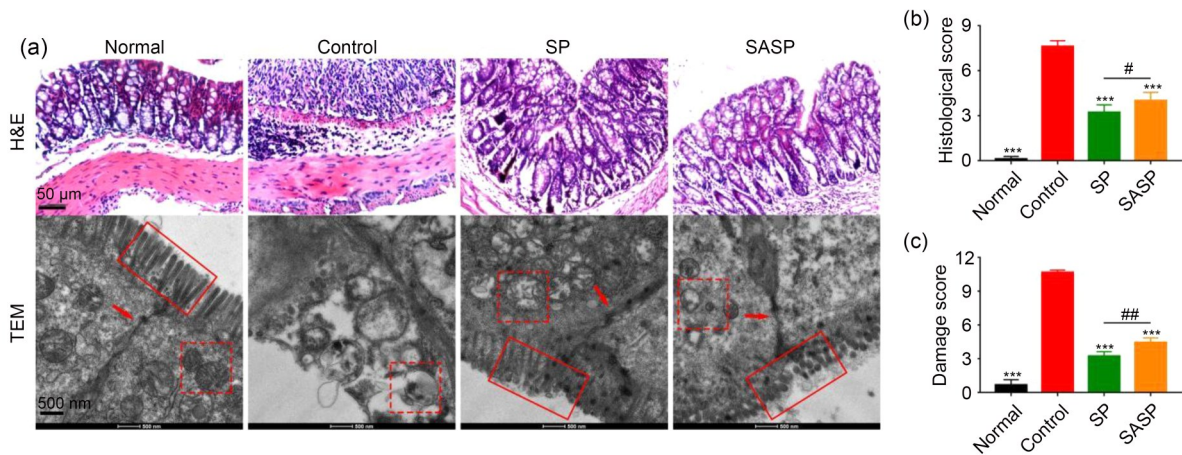


**Fig. 7** Positive effect of SP on pathological structure damage of colon in DSS-treated mice. (a) Representative photomicrographs and TEM ultrastructure images of colon sections. Red arrows: the tight junctions; Red dashed frames: the intracellular substances; Red solid frames: the colonic microvilli. (b) Histological damage score. (c) Damage score. Data are expressed as mean±standard deviation ( $n=6$ ). \*\*\*  $P<0.001$ , compared with the control group; #  $P<0.05$ , ##  $P<0.01$ , compared between the SP and SASP groups. TEM: transmission electron microscopy; H&E: hematoxylin and eosin; SASP: sulfasalazine; SP: *Spirulina platensis* aqueous extracts; DSS: dextran sulfate sodium.

pathology were analyzed in serum samples and colon tissues (Fig. 8). Compared with the control group, there was a significant decrease in the levels of TNF- $\alpha$ ,

IFN- $\gamma$ , IL-6, IL-1 $\beta$ , IL-17, and DAO upon treatment with SP. In contrast, the concentration of the anti-inflammatory cytokine IL-10 was higher than that in

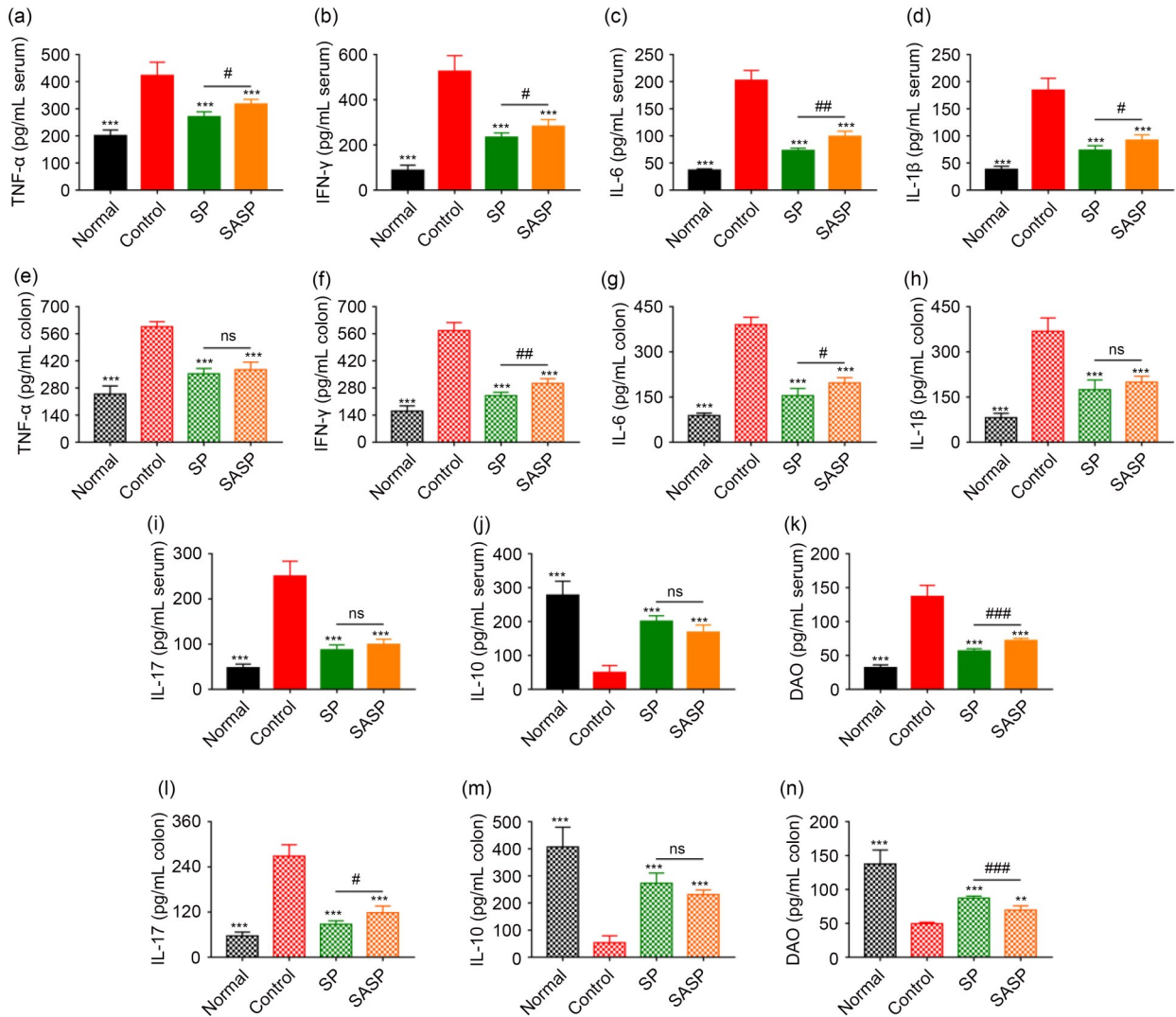


**Fig. 8** Effects of SP on the expression of inflammatory cytokines in serum (a–d, i–k) and colon (e–h, l–n). Data are expressed as mean±standard deviation ( $n=6$ ). \*\*  $P<0.01$ , \*\*\*  $P<0.001$ , compared with the control group; #  $P<0.05$ , ##  $P<0.01$ , ###  $P<0.001$ , ns No significant difference, compared between the SP and SASP groups. TNF- $\alpha$ : tumor necrosis factor- $\alpha$ ; IFN- $\gamma$ : interferon- $\gamma$ ; IL: interleukin; DAO: diamine oxidase; SASP: sulfasalazine; SP: *Spirulina platensis* aqueous extracts.

the control group. In summary, SP attenuated the DSS-induced inflammation in the serum and colon.

### 3.6 Attenuated oxidative stress in colon tissues upon SP treatment

Oxidative stress factors are important indices for evaluating the health of colon epithelial tissue (Payne et al., 2007). The levels of oxidative stress factors in colon tissues were measured to determine the protective function of SP against oxidative stress. SP treatment significantly increased the activity of SOD, CAT, and GSH-Px compared with those seen in the control

group, in addition to strikingly inhibiting MPO activity and MDA levels in colon tissues (Fig. 9).

### 3.7 Regulation of the transcriptional expression of genes and protein associated with intestinal TJs and inflammation by SP

qPCR detection was used to evaluate the effect of SP on the mRNA expression levels of colonic TJs (ZO-1, claudin-1, and occludin) and inflammation-associated proteins (NF- $\kappa$ B p65, COX-2, and iNOS) (Fig. 10). Compared with the control group, SP significantly increased the mRNA expression of ZO-1,

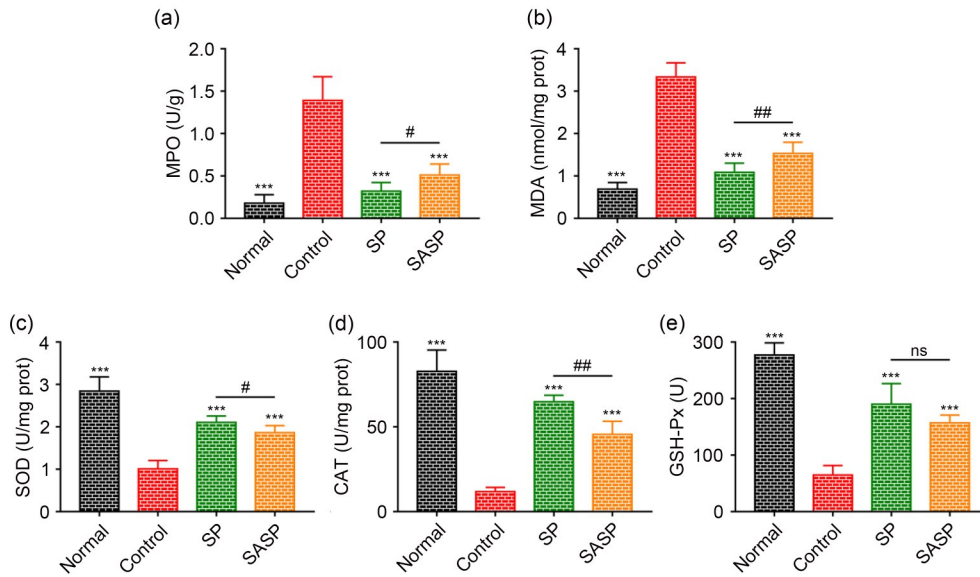


**Fig. 9** The activity of MPO (a), SOD (c), CAT (d), and GSH-Px (e) and the content of MDA (b) in mice colon tissues among four groups with colitis. Data are expressed as mean±standard deviation ( $n=6$ ). \*\*\*  $P<0.001$ , compared with the control group; #  $P<0.05$ , ##  $P<0.01$ , ns No significant difference, compared between the SP and SASP groups. MPO: myeloperoxidase; MDA: malondialdehyde; SOD: superoxide dismutase; CAT: catalase; GSH-Px: glutathione peroxidase; prot: protein; SASP: sulfasalazine; SP: *Spirulina platensis* aqueous extracts.

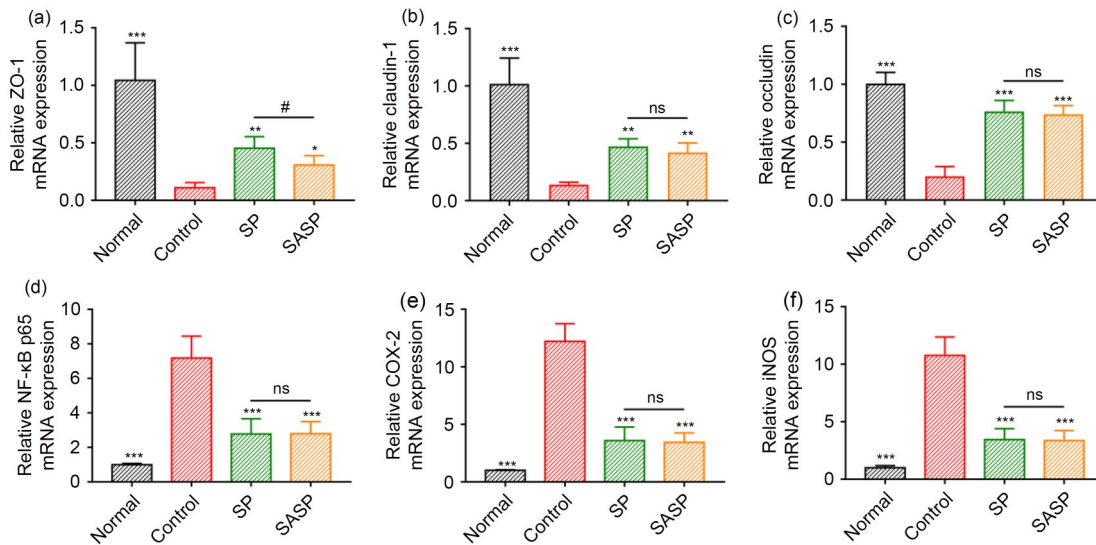


**Fig. 10** Relative mRNA expression of ZO-1 (a), claudin-1 (b), occludin (c), NF-κB p65 (d), COX-2 (e), and iNOS (f) in colon tissues. Data are expressed as mean±standard deviation ( $n=6$ ). \*  $P<0.05$ , \*\*  $P<0.01$ , \*\*\*  $P<0.001$ , compared with the control group; #  $P<0.05$ , ns No significant difference, compared between the SP and SASP groups. mRNA: messenger RNA; ZO-1: zonula occludens-1; NF-κB: nuclear factor-κB; COX-2: cyclooxygenase-2; iNOS: inducible nitric oxide synthase; SASP: sulfasalazine; SP: *Spirulina platensis* aqueous extracts.

claudin-1, and occludin, and markedly inhibited the expression of NF-κB p65, COX-2, and iNOS. The results of the western blot were consistent with those of the qPCR (Fig. 11). Hence, SP could protect the gut barrier function by preserving TJ integrity and inhibiting inflammation in colon tissues.

### 3.8 Modulation of the composition of gut microbiota by SP

To investigate whether SP could regulate gut microbiota, we performed 16S rDNA high-throughput sequencing to determine the changes in the intestinal

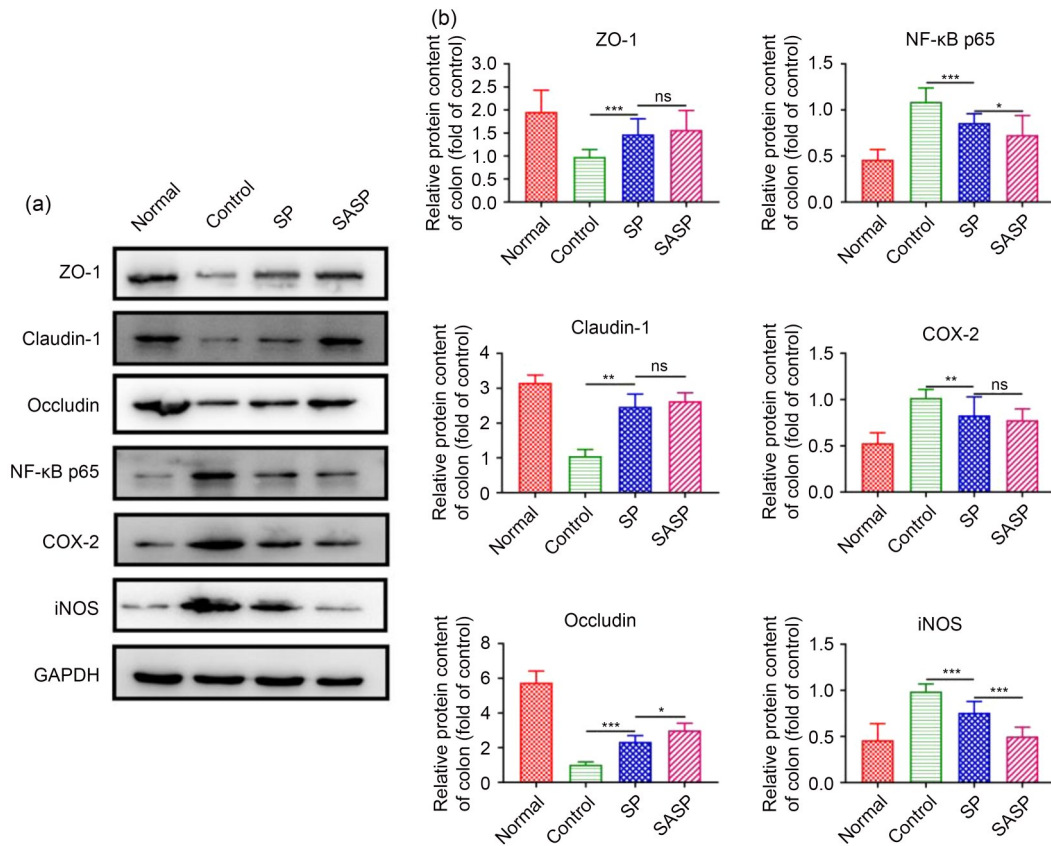


**Fig. 11** Effects of SP on the protein expression in four groups, with GAPDH as a loading control (a) and corresponding statistical graphs (b). Values are expressed as mean±standard deviation ( $n=6$ ). \*  $P<0.05$ , \*\*  $P<0.01$ , \*\*\*  $P<0.001$ , ns No significant difference. ZO-1: zonula occludens-1; NF-κB: nuclear factor-κB; COX-2: cyclooxygenase-2; iNOS: inducible nitric oxide synthase; GAPDH: glyceraldehyde-3-phosphate dehydrogenase; SASP: sulfasalazine; SP: *Spirulina platensis* aqueous extracts.

microbiome composition among the four groups. The ten most abundant bacteria at the phylum and genus levels were compared among the groups (Figs. 12a and 12b). The composition of intestinal bacterial species in the SP group changed dramatically compared with that in the control group. The abundance of Firmicutes increased in the SP group, with the same trend as in the SASP group. Among the ten most abundant bacteria at the genus level, SP treatment increased the abundance of *Romboutsia* and *Stenotrophomonas*. Heatmap and cluster analyses were conducted based on the 35 species most abundant at the genus level (Fig. 12c). SP substantially increased the relative abundance of *Akkermansia*, *Romboutsia*, *Sphingomonas*, *Helcococcus*, *Atopostipes*, *Alistipes*, *Anaerococcus*, *Stenotrophomonas*, *Corynebacterium*, *Streptococcus*, and *Vagococcus*. Unweighted UniFrac-based principal coordinates analysis (PCoA) revealed a distinct clustering of microbiota composition for each group, and

a lower sample distance implied a similar species composition. The normal group was relatively close to the SP group cluster (Fig. 12d). Non-metric multidimensional scaling (NMDS) and *t*-test analyses were used to detect significant differences among the different groups (Figs. 12e–12g). NMDS analysis based on OTU level reflected the inter- and intra-group differences in the samples in terms of the distance between points, and showed that the species composition of intestinal flora in the SP group was closer to that of the normal group than that of the control group. The *t*-test analysis indicated that the species composition of intestinal flora in the SP group was different from that in the control group. SP significantly improved the relative abundance of Firmicutes at the phylum level, with a reduced relative abundance of unidentified Enterobacteriaceae at the genus level. Based on the unweighted pair group method with arithmetic mean (UPGMA) clustering tree (Fig. 12h), the community

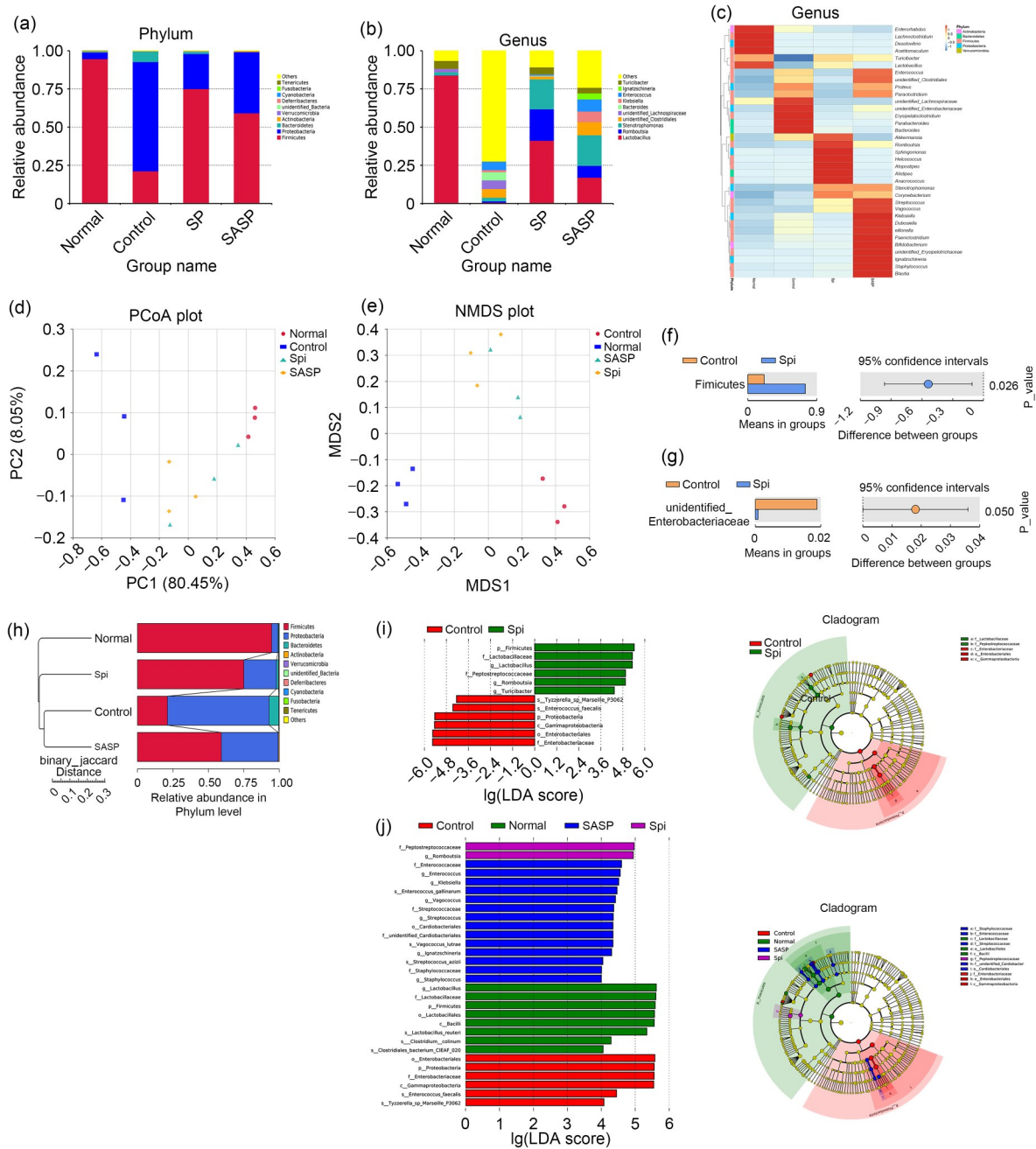


**Fig. 12** SP dietary supplementation effect on gut microbiome structure and composition ( $n=3$ ). (a, b) Relative abundance of top 10 species at phylum and genus level. (c) Species abundance of top 35 species at the genus level; the left side of the cluster tree represents the species cluster tree. (d, e) Unweighted UniFrac-based PCoA, each point represents a sample; dots with the same color indicate samples in the same group, which is consistent with NMDS analysis. When the stress is less than 0.2, NMDS could reflect the difference between samples. (f, g) Inter-group species difference analyses by  $t$ -tests. (h) UPGMA clustering tree. (i, j) LDA plots highlighting significantly differences in characteristic taxa between microbiota of control and SP groups; only those taxa with an LDA score more than 4 were considered. Taxonomic cladogram of bacterial fecal samples from all groups. SASP: sulfasalazine; SP: *Spirulina platensis* aqueous extracts; Spi: SP group; PCoA: principal coordinates analysis; NMDS: non-metric multidimensional scaling; UPGMA: unweighted pair group method with arithmetic mean; LDA: linear discriminant analysis.

structure of the SP group was similar to those of the SASP and normal groups, but distinct from that of the

control group, indicating that SP exerted considerable positive effects on the intestinal flora. LEfSe analysis

(Figs. 12i and 12j) demonstrated that SP increased the relative proportions of the following bacteria: phylum Firmicutes, family Lactobacillaceae and Peptostreptococcaceae, genus *Lactobacillus*, *Romboutsia*, and *Turicibacter*. In the control group, the greatest growth was shown by the phylum Proteobacteria, class Gammaproteobacteria, order Enterobacteriales, family Enterobacteriaceae. Moreover, the cladogram showed that in the SP group, Lactobacillaceae and Peptostreptococcaceae were primarily enriched at the family level. The cladogram corroborated the LEfSe analysis results for the normal and SP groups.

### 3.9 Relationship between the amelioration of intestinal flora imbalance by SP and the enhancement of antioxidant enzyme activity and TJs in colon tissues

Spearman's sequential correlation analysis was conducted at the phylum and genus levels to investigate the relationship between the intestinal microbiome and biochemical indicators. At the phylum level (Fig. 13a), Firmicutes were positively correlated with antioxidant enzymes, and Proteobacteria were negatively correlated with antioxidant enzymes, but positively correlated with inflammatory cytokine indicators. At the genus level, unidentified Enterobacteriaceae, *Dubosiella*, *Enterococcus*, *Klebsiella*, and unidentified Clostridiales were positively correlated with inflammatory cytokine indicators and negatively correlated with antioxidant enzymes. Species at the phylum level (Fig. 13b), including Fusobacteria and Cyanobacteria, were positively correlated with ZO-1, claudin-1, and occludin, but negatively correlated with NF- $\kappa$ B p65, COX-2, and iNOS. At the genus level, *Corynebacterium*, *Proteus*, *Veillonella*, *Vagococcus*, *Bifidobacterium*, unidentified Erysipelotrichaceae, *Pae-niclostridium*, *Blautia*, *Staphylococcus*, *Dubosiella*, *Streptococcus*, *Ignatzschineria*, *Enterococcus*, *Klebsi-ella*, unidentified Clostridiales, *Stenotrophomonas*, and *Romboutsia* were positively correlated with ZO-1, claudin-1, and occludin. However, *Acetitomaculum*, *Enterorhabdus*, *Lachnoclostridium*, and *Desulfovibrio* were positively correlated with NF- $\kappa$ B p65, COX-2, and iNOS. In summary, much of the improvement in the intestinal flora following SP treatment may have been achieved by increasing the activity of antioxidant enzymes and TJs in the colon.

## 4 Discussion

Numerous studies have concluded that edible plants are of pivotal importance for the treatment of colonic inflammation in various experimental colitis murine models (Vinolo et al., 2011; Speckmann and Steinbrenner, 2014; Zarepoor et al., 2014). *S. platensis* products have been widely used as functional foods because of their high protein content and other nutritional features (Szulinska et al., 2017; Yousefi et al., 2019). However, very little research has focused on the effects of SP on colonic mucosal damage and gut microbiota disorders in UC mice. Our results suggested that oral administration of SP led to a significant reduction in the severity of colon injury and gut microbiota disorders, in terms of symptoms such as diarrhea, weight loss, hematochezia, and colon shortening. Moreover, SP supplementation inhibited inflammation, oxidative stress response, and colonic epithelial cell injury, while preserving TJs. Most importantly, SP ameliorated gut microbiota disorders, mainly by increasing antioxidant enzyme activity and the expression of TJs in colon tissues.

Apoptosis, also known as programmed cell death, is regulated by a variety of genes and proteins. Abnormal cell apoptosis promotes the development of diseases (Xue et al., 2020). Colonic epithelial cell apoptosis is an important characteristic of UC. Mitochondria are the main regulators of the mitochondria-mediated apoptosis pathway, and mitochondrial dysfunction is closely related to apoptotic signals (Kariyil et al., 2021). Oxidative damage is characterized by the overproduction of ROS in cells or tissues, and abnormal apoptosis mediated by oxidative stress apparently increases the potential risk of cancer (Bradley et al., 1982; Zhang et al., 2019). In our in vitro studies, DSS-induced NCM460 cell apoptosis was confirmed, and the potential therapeutic mechanism of SP was evaluated. The results proved that SP attenuated DSS-induced NCM460 cell apoptosis by inhibiting ROS-mediated oxidative damage and mitochondrial dysfunction.

The DSS-induced colitis model is a well-established and widely used model that has been applied to study UC in mice, because the disease in this model has a great deal of similarity with human UC (Taghipour et al., 2019; Nielsen et al., 2020). These similarities are in terms of symptoms of UC such as body weight loss, diarrhea, hematochezia, shorter



pro-inflammatory mediators, thus reflecting the degree of inflammation. The large amount of nitric oxide generated by iNOS directly or indirectly causes damage to the mucosal barrier and stimulates inflammation (Unno et al., 1997). In this study, there was an increase in the mRNA and protein levels of NF- $\kappa$ B p65, COX-2, and iNOS in the colon tissues post-DSS treatment. However, SP treatment significantly suppressed this adverse trend. Therefore, we conclude that SP inhibited inflammation in the colon tissues of the UC mice.

The number of goblet cells and the appearance of mucus-producing defects are reduced in UC-afflicted colon tissues (Castro-Ochoa et al., 2019). Thus, maintaining the tightness and integrity of the mucus barrier associated with goblet cells is also a vital target in the treatment of UC. The abnormal loss of three TJs, ZO-1, occludin, and claudin-1, may also impair the colon epithelial barrier. ZO-1 is associated with intestinal epithelial integrity and is regarded as a marker of the condition of the gut mechanical barrier. Occludin plays an important role in barrier function and TJ stability. Claudin-1 is an integral membrane protein that is also involved in the composition of TJs (Sun et al., 2020a). H&E staining and TEM results showed that SP significantly restored the number of goblet cells and alleviated TJ damage, thereby maintaining the integrity of the colonic barrier. These results were confirmed by qPCR and western blot.

In the initiation and progression of UC, oxidative stress often plays a fundamental role (Yusuf et al., 2016). The infiltration of inflammatory cells triggers free radical production, which then destroys the endogenous defense systems and epithelial cell integrity, induces intestinal mucosal immune dysfunction, and delays intestinal mucosal recovery. MPO activity often increases in the inflamed mucosa of gastrointestinal tissues, which is in accordance with the results of this study. DSS-induced oxidative stress and lipid peroxidation were also indicated by the increase in MDA content and the decrease in activity of GSH-Px, SOD, and CAT (the important antioxidant enzymes in defense against intestinal injury). As expected, SP had a positive effect on oxidative stress in the process of colon injury induced by DSS, by enhancing antioxidant enzyme activity and reducing MPO activity and MDA content.

Gut microbiota disorder has long been recognized as a key problem in the pathogenesis of UC

(Guinane and Cotter, 2013). The gut microbiota plays an indispensable role in the maintenance of the host immune system via its symbiotic relationship with immune cells (Laparra and Sanz, 2010; Hayes et al., 2018). Many dietary components or functional foods have an impact on the gut microbiota, and their potential functions in preventing UC have been investigated. In this study, DSS-induced colitis was found to lead to a negative change in the composition of intestinal microflora. Intestinal microflora dysbiosis further aggravated the colon barrier injury. However, a positive reversal occurred upon SP treatment. Our results demonstrated that SP significantly improved the species abundance, altered the microbiota composition, and increased the populations of beneficial intestinal microflora (Fig. 14). Although SP may have caused an increase in the number of pathogenic bacteria, overall its positive effects were far greater than its negative effects. Spearman's correlation analysis revealed that SP ameliorated the intestinal flora imbalance, primarily through enhancing antioxidant enzyme activity and TJs in colon tissues.

## 5 Conclusions

In conclusion, our findings revealed that SP ameliorates colonic mucosal damage and modulates gut microbiota disorders in mice with UC. The protective effect of SP against UC is mediated through a reduction in inflammatory cytokine overproduction, oxidative stress inhibition, and enhanced expression of TJs in the colonic mucosa barrier. Therefore, SP could serve as an attractive natural antioxidant for therapy of UC or other gut microbiota disorders and oxidative stress-associated diseases.

## Acknowledgments

This work was supported by the National Key R&D Program of China (No. 2018YFC1603900), the National Natural Science Foundation of China (Nos. 32070509 and 31501894), and the Guangdong Basic and Applied Basic Research Foundation (No. 2021A1515220119), China.

## Author contributions

Jian WANG and Liqian SU performed the experimental research and data analysis. Jian WANG wrote and edited the manuscript. Lun ZHANG, Jiali ZENG, Qingru CHEN, Rui DENG, Ziyang WANG, and Weidong KUANG established the

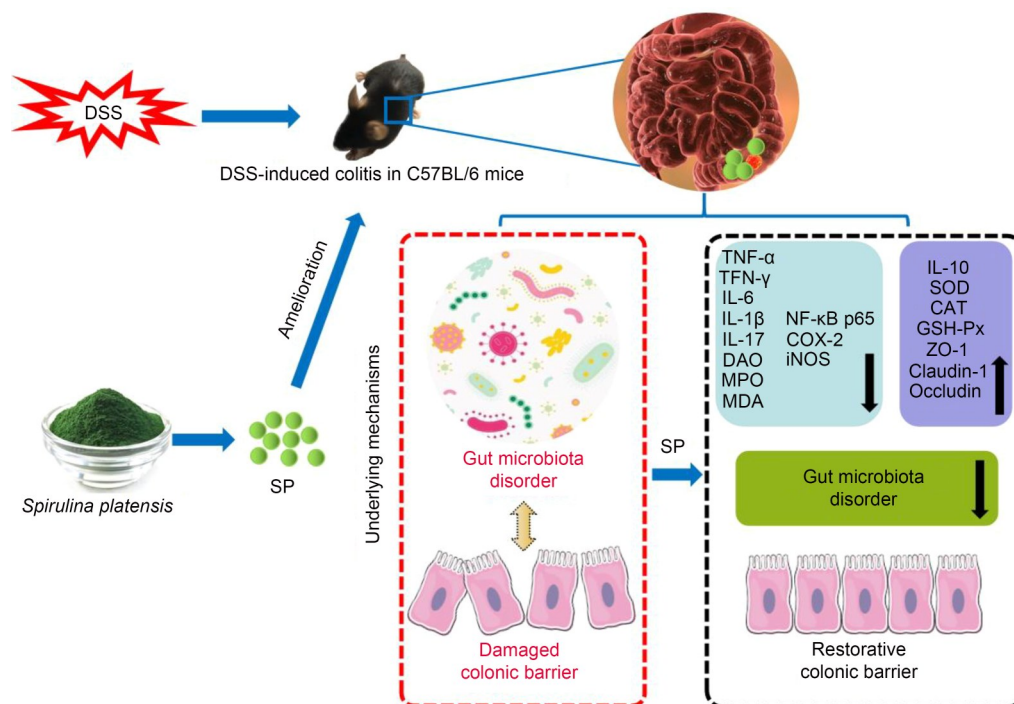


**Fig. 14** Summary of the protective effects of SP against DSS-induced colitis through a reduction in inflammatory cytokine overproduction, inhibition oxidative stress, and enhanced expression of TJs in the colonic mucosa barrier and modulated gut microbiota disorder. SP: *Spirulina platensis* aqueous extracts; DSS: dextran sulfate sodium; TJs: tight junction proteins; TNF- $\alpha$ : tumor necrosis factor- $\alpha$ ; IFN- $\gamma$ : interferon- $\gamma$ ; IL: interleukin; DAO: diamine oxidase; MPO: myeloperoxidase; MDA: malondialdehyde; NF- $\kappa$ B: nuclear factor- $\kappa$ B; COX-2: cyclooxygenase-2; iNOS: inducible nitric oxide synthase; SOD: superoxide dismutase; CAT: catalase; GSH-Px: glutathione peroxidase; ZO-1: zonula occludens-1.

animal models. Xiaobao JIN, Shuiqing GUI, Yinghua XU, and Xuemei LU contributed to the study design, data analysis, and article revision. All authors have read and approved the final manuscript, and therefore, have full access to all the data in the study and take responsibility for the integrity and security of the data.

### Compliance with ethics guidelines

Jian WANG, Liqian SU, Lun ZHANG, Jiali ZENG, Qingru CHEN, Rui DENG, Ziyang WANG, Weidong KUANG, Xiaobao JIN, Shuiqing GUI, Yinghua XU, and Xuemei LU declare that they have no conflict of interest.

All institutional and national guidelines for the care and use of laboratory animals were followed. The study complied with the Guidelines for the Care and Use of Experimental Animals, Guangdong Pharmaceutical University (No. SYXK (Yue) 2012-0125) and was approved by the Guangdong Pharmaceutical University Animal Care and Use Committee, China.

### References

Akimoto T, Takasawa A, Murata M, et al., 2016. Analysis of the expression and localization of tight junction transmembrane proteins, claudin-1, -4, -7, occludin and JAM-A, in

human cervical adenocarcinoma. *Histol Histopathol*, 31(8): 921-931.

<https://doi.org/10.14670/HH-11-729>

Alwaleed EA, El-Sheekh M, Abdel-Daim MM, et al., 2021. Effects of *Spirulina platensis* and *Amphora coffeaeformis* as dietary supplements on blood biochemical parameters, intestinal microbial population, and productive performance in broiler chickens. *Environ Sci Pollut Res Int*, 28(2):1801-1811.

<https://doi.org/10.1007/s11356-020-10597-3>

Berruén NNA, Smith CL, 2020. Emerging roles of melanocortin receptor accessory proteins (MRAP and MRAP2) in physiology and pathophysiology. *Gene*, 757:144949.

<https://doi.org/10.1016/j.gene.2020.144949>

Betanzos A, Javier-Reyna R, Garcia-Rivera G, et al., 2013. The EhCPADH112 complex of *Entamoeba histolytica* interacts with tight junction proteins occludin and claudin-1 to produce epithelial damage. *PLoS ONE*, 8(6):e65100.

<https://doi.org/10.1371/journal.pone.0065100>

Bradley PP, Priebe DA, Christensen RD, et al., 1982. Measurement of cutaneous inflammation: estimation of neutrophil content with an enzyme marker. *J Invest Dermatol*, 78(3):206-209.

<https://doi.org/10.1111/1523-1747.ep12506462>

Cani PD, Possemiers S, van de Wiele T, et al., 2009. Changes

- in gut microbiota control inflammation in obese mice through a mechanism involving GLP-2-driven improvement of gut permeability. *Gut*, 58(8):1091-1103. <https://doi.org/10.1136/gut.2008.165886>
- Castro-Ochoa KF, Vargas-Robles H, Cháñez-Paredes S, et al., 2019. Homoectoine protects against colitis by preventing a claudin switch in epithelial tight junctions. *Dig Dis Sci*, 64(2):409-420. <https://doi.org/10.1007/s10620-018-5309-8>
- Ciapetti G, Cenni E, Pratelli L, et al., 1993. *In vitro* evaluation of cell/biomaterial interaction by MTT assay. *Bio-materials*, 14(5):359-364. [https://doi.org/10.1016/0142-9612\(93\)90055-7](https://doi.org/10.1016/0142-9612(93)90055-7)
- da Cunha VP, Preisser TM, Santana MP, et al., 2020. Invasive *Lactococcus lactis* producing mycobacterial Hsp65 ameliorates intestinal inflammation in acute TNBS-induced colitis in mice by increasing the levels of the cytokine IL-10 and secretory IgA. *J Appl Microbiol*, 129(5):1389-1401. <https://doi.org/10.1111/jam.14695>
- Davaatseren M, Hwang JT, Park JH, et al., 2014. Allyl isothiocyanate ameliorates angiogenesis and inflammation in dextran sulfate sodium-induced acute colitis. *PLoS ONE*, 9(7):e102975. <https://doi.org/10.1371/journal.pone.0102975>
- Ding SJ, Ma Y, Liu G, et al., 2019. *Lactobacillus brevis* alleviates DSS-induced colitis by reprogramming intestinal microbiota and influencing serum metabolome in murine model. *Front Physiol*, 10:1152. <https://doi.org/10.3389/fphys.2019.01152>
- Dobi A, Rosanaly S, Devin A, et al., 2021. Advanced glycation end-products disrupt brain microvascular endothelial cell barrier: the role of mitochondria and oxidative stress. *Microvasc Res*, 133:104098. <https://doi.org/10.1016/j.mvr.2020.104098>
- Echele DD, Kharbanda KK, 2017. Dextran sodium sulfate colitis murine model: an indispensable tool for advancing our understanding of inflammatory bowel diseases pathogenesis. *World J Gastroenterol*, 23(33):6016-6029. <https://doi.org/10.3748/wjg.v23.i33.6016>
- Emamie AD, Rajabpour M, Ghanavati R, et al., 2021. The effects of probiotics, prebiotics and synbiotics on the reduction of IBD complications, a periodic review during 2009–2020. *J Appl Microbiol*, 130(6):1823-1838. <https://doi.org/10.1111/jam.14907>
- Eray M, Mättö M, Kaartinen M, et al., 2001. Flow cytometric analysis of apoptotic subpopulations with a combination of annexin V-FITC, propidium iodide, and SYTO 17. *Cytometry*, 43(2):134-142. [https://doi.org/10.1002/1097-0320\(20010201\)43:2<134::AID-CYTO1028>3.0.CO;2-L](https://doi.org/10.1002/1097-0320(20010201)43:2<134::AID-CYTO1028>3.0.CO;2-L)
- Guinane CM, Cotter PD, 2013. Role of the gut microbiota in health and chronic gastrointestinal disease: understanding a hidden metabolic organ. *Therap Adv Gastroenterol*, 6(4):295-308. <https://doi.org/10.1177/1756283X13482996>
- Halfvarson J, Brislawn CJ, Lamendella R, et al., 2017. Dynamics of the human gut microbiome in inflammatory bowel disease. *Nat Microbiol*, 2(5):17004. <https://doi.org/10.1038/nmicrobiol.2017.4>
- Hayes CL, Dong J, Galipeau HJ, et al., 2018. Commensal microbiota induces colonic barrier structure and functions that contribute to homeostasis. *Sci Rep*, 8:14184. <https://doi.org/10.1038/s41598-018-32366-6>
- Ida N, Hartmann T, Pantel J, et al., 1996. Analysis of heterogeneous  $\beta$ A4 peptides in human cerebrospinal fluid and blood by a newly developed sensitive western blot assay. *J Biol Chem*, 271(37):22908-22914. <https://doi.org/10.1074/jbc.271.37.22908>
- Kaplan GG, 2015. The global burden of IBD: from 2015 to 2025. *Nat Rev Gastroenterol Hepatol*, 12(12):720-727. <https://doi.org/10.1038/nrgastro.2015.150>
- Kariyil BJ, Ayyappan UPT, Gopalakrishnan A, et al., 2021. Chloroform fraction of methanolic extract of seeds of *Annona muricata* induce S phase arrest and ROS dependent caspase activated mitochondria-mediated apoptosis in triple-negative breast cancer. *Anticancer Agents Med Chem*, 21(10):1250-1265. <https://doi.org/10.2174/1871520620666200918101448>
- Kose A, Ozen MO, Elibol M, et al., 2017. Investigation of in vitro digestibility of dietary microalga *Chlorella vulgaris* and cyanobacterium *Spirulina platensis* as a nutritional supplement. *3 Biotech*, 7(3):170. <https://doi.org/10.1007/s13205-017-0832-4>
- Kruidenier L, Kuiper I, Lamers CB, et al., 2003. Intestinal oxidative damage in inflammatory bowel disease: semi-quantification, localization, and association with mucosal antioxidants. *J Pathol*, 201(1):28-36. <https://doi.org/10.1002/path.1409>
- Laparra JM, Sanz Y, 2010. Interactions of gut microbiota with functional food components and nutraceuticals. *Pharmacol Res*, 61(3):219-225. <https://doi.org/10.1016/j.phrs.2009.11.001>
- Li LH, Yang F, Jia RJ, et al., 2020. Velvet antler polypeptide prevents the disruption of hepatic tight junctions via inhibiting oxidative stress in cholestatic mice and liver cell lines. *Food Funct*, 11(11):9752-9763. <https://doi.org/10.1039/d0fo01899f>
- Liu QQ, Zeng XL, Guan YL, et al., 2020. Verticillin A inhibits colon cancer cell migration and invasion by targeting *c-Met*. *J Zhejiang Univ-Sci B (Biomed & Biotechnol)*, 21(10):779-795. <https://doi.org/10.1631/jzus.B2000190>
- Lu J, Chen XN, Xu XH, et al., 2019. Active polypeptides from *Hirudo* inhibit endothelial cell inflammation and macrophage foam cell formation by regulating the LOX-1/LXR- $\alpha$ /ABCA1 pathway. *Biomed Pharmacother*, 115:108840. <https://doi.org/10.1016/j.biopha.2019.108840>
- Luo M, Luo Y, 2021. Imperatorin relieved ulcerative colitis by regulating the Nrf-2/ARE/HO-1 pathway in rats. *Inflammation*, 44(2):558-569. <https://doi.org/10.1007/s10753-020-01353-3>
- Mishra SK, Kang JH, Kim DK, et al., 2012. Orally administered aqueous extract of *Inonotus obliquus* ameliorates acute inflammation in dextran sulfate sodium (DSS)-induced colitis in mice. *J Ethnopharmacol*, 143(2):524-532.

- <https://doi.org/10.1016/j.jep.2012.07.008>
- Nielsen TS, Fredborg M, Theil PK, et al., 2020. Dietary red meat adversely affects disease severity in a pig model of DSS-induced colitis despite reduction in colonic pro-inflammatory gene expression. *Nutrients*, 12(6):1728. <https://doi.org/10.3390/nu12061728>
- Pardhasaradhi BVV, Ali AM, Kumari AL, et al., 2003. Phycocyanin-mediated apoptosis in AK-5 tumor cells involves down-regulation of Bcl-2 and generation of ROS. *Mol Cancer Ther*, 2(11):1165-1170.
- Park JH, Lee SI, Kim IH, 2018. Effect of dietary *Spirulina (Arthrospira) platensis* on the growth performance, antioxidant enzyme activity, nutrient digestibility, cecal microflora, excreta noxious gas emission, and breast meat quality of broiler chickens. *Poult Sci*, 97(7):2451-2459. <https://doi.org/10.3382/ps/pey093>
- Payne CM, Weber C, Crowley-Skillicorn C, et al., 2007. Deoxycholate induces mitochondrial oxidative stress and activates NF- $\kappa$ B through multiple mechanisms in HCT-116 colon epithelial cells. *Carcinogenesis*, 28(1):215-222. <https://doi.org/10.1093/carcin/bgl139>
- Prasad A, Pospisil P, Tada M, 2019. Editorial: reactive oxygen species (ROS) detection methods in biological system. *Front Physiol*, 10:1316. <https://doi.org/10.3389/fphys.2019.01316>
- Rao XY, Huang XL, Zhou ZC, et al., 2013. An improvement of the  $2^(-\Delta\Delta CT)$  method for quantitative real-time polymerase chain reaction data analysis. *Biostat Bioinforma Biomath*, 3(3):71-85.
- Reers M, Smiley ST, Mottola-Hartshorn C, et al., 1995. Mitochondrial membrane potential monitored by JC-1 dye. *Methods Enzymol*, 260:406-414, IN1-IN3, 415-417. [https://doi.org/10.1016/0076-6879\(95\)60154-6](https://doi.org/10.1016/0076-6879(95)60154-6)
- Siddiqui H, Nederbragt AJ, Lagesen K, et al., 2011. Assessing diversity of the female urine microbiota by high throughput sequencing of 16S rDNA amplicons. *BMC Microbiol*, 11:244. <https://doi.org/10.1186/1471-2180-11-244>
- Sokol H, Beaugerie L, 2010. Body mass index and disease activity at treatment initiation: potential new predictors of response to azathioprine therapy in IBD. *Inflamm Bowel Dis*, 16(4):714-715. <https://doi.org/10.1002/ibd.21102>
- Speckmann B, Steinbrenner H, 2014. Selenium and selenoproteins in inflammatory bowel diseases and experimental colitis. *Inflamm Bowel Dis*, 20(6):1110-1119. <https://doi.org/10.1097/MIB.000000000000020>
- Sun Y, Ge X, Li X, et al., 2020a. High-fat diet promotes renal injury by inducing oxidative stress and mitochondrial dysfunction. *Cell Death Dis*, 11(10):914. <https://doi.org/10.1038/s41419-020-03122-4>
- Sun Y, Li LW, Lai AY, et al., 2020b. Does ulcerative colitis influence the inter-individual heterogeneity of the human intestinal mucosal microbiome? *Evol Bioinform*, 16:1176934320948848. <https://doi.org/10.1177/1176934320948848>
- Szulinska M, Gibas-Dorna M, Miller-Kasprzak E, et al., 2017. *Spirulina maxima* improves insulin sensitivity, lipid profile, and total antioxidant status in obese patients with well-treated hypertension: a randomized double-blind placebo-controlled study. *Eur Rev Med Pharmacol Sci*, 21(10):2473-2481.
- Taghipour N, Mosaffa N, Aghdaei HA, et al., 2019. Immunomodulatory effect of *Syphacia obvelata* in treatment of experimental DSS-induced colitis in mouse model. *Sci Rep*, 9:19127. <https://doi.org/10.1038/s41598-019-55552-6>
- Takagi T, Naito Y, Uchiyama K, et al., 2011. Carbon monoxide liberated from carbon monoxide-releasing molecule exerts an anti-inflammatory effect on dextran sulfate sodium-induced colitis in mice. *Dig Dis Sci*, 56(6):1663-1671. <https://doi.org/10.1007/s10620-010-1484-y>
- Tsang L, Banerjee N, Tabibian JH, 2019. Bloody diarrhea and weight loss in a patient in remission from ulcerative colitis. *Gastroenterology*, 157(5):1207-1209. <https://doi.org/10.1053/j.gastro.2019.01.272>
- Unno N, Wang H, Menconi MJ, et al., 1997. Inhibition of inducible nitric oxide synthase ameliorates endotoxin-induced gut mucosal barrier dysfunction in rats. *Gastroenterology*, 113(4):1246-1257. <https://doi.org/10.1053/gast.1997.v113.pm9322519>
- Vinolo MAR, Rodrigues HG, Nachbar RT, et al., 2011. Regulation of inflammation by short chain fatty acids. *Nutrients*, 3(10):858-876. <https://doi.org/10.3390/nu3100858>
- Wargo JA, 2020. Modulating gut microbes. *Science*, 369(6509):1302-1303. <https://doi.org/10.1126/science.abc3965>
- Xu LL, Liu T, Wang L, et al., 2018. 3-(1H-Benzo[d]imidazol-6-yl)-5-(4-fluorophenyl)-1,2,4-oxadiazole (DDO7232), a novel potent Nrf2/ARE inducer, ameliorates DSS-induced murine colitis and protects NCM460 cells against oxidative stress via ERK1/2 phosphorylation. *Oxid Med Cell Longev*, 2018:3271617. <https://doi.org/10.1155/2018/3271617>
- Xue PP, Wang LF, Xu JW, et al., 2020. Temperature-sensitive hydrogel for rectal perfusion improved the therapeutic effect of Kangfuxin liquid on DSS-induced ulcerative colitis mice: the inflammation alleviation and the colonic mucosal barriers repair. *Int J Pharm*, 589:119846. <https://doi.org/10.1016/j.ijpharm.2020.119846>
- Ye ZH, Ning K, Ander BP, et al., 2020. Therapeutic effect of methane and its mechanism in disease treatment. *J Zhejiang Univ-Sci B (Biomed & Biotechnol)*, 21(8):593-602. <https://doi.org/10.1631/jzus.B1900629>
- Yousefi R, Saidpour A, Mottaghi A, 2019. The effects of *Spirulina* supplementation on metabolic syndrome components, its liver manifestation and related inflammatory markers: a systematic review. *Complement Ther Med*, 42:137-144. <https://doi.org/10.1016/j.ctim.2018.11.013>
- Yusuf MS, Hassan MA, Abdel-Daim MM, et al., 2016. Value added by *Spirulina platensis* in two different diets on growth performance, gut microbiota, and meat quality of Japanese quails. *Vet World*, 9(11):1287-1293. <https://doi.org/10.14202/vetworld.2016.1287-1293>
- Zarepoor L, Lu JT, Zhang C, et al., 2014. Dietary flaxseed

- intake exacerbates acute colonic mucosal injury and inflammation induced by dextran sodium sulfate. *Am J Physiol Gastrointest Liver Physiol*, 306(12):G1042-G1055. <https://doi.org/10.1152/ajpgi.00253.2013>
- Zhang FX, Wu WM, Deng ZY, et al., 2015. High altitude increases the expression of hypoxia-inducible factor 1 $\alpha$  and inducible nitric oxide synthase with intestinal mucosal barrier failure in rats. *Int J Clin Exp Pathol*, 8(5):5189-5195.
- Zhang L, Gui SQ, Liang ZB, et al., 2019. *Musca domestica* cecropin (Mdc) alleviates *Salmonella typhimurium*-induced colonic mucosal barrier impairment: associating with inflammatory and oxidative stress response, tight junction as well as intestinal flora. *Front Microbiol*, 10:522. <https://doi.org/10.3389/fmicb.2019.00522>
- Zhang L, Gui SQ, Xu YH, et al., 2021. Colon tissue-accumulating mesoporous carbon nanoparticles loaded with *Musca domestica* cecropin for ulcerative colitis therapy. *Theranostics*, 11(7):3417-3438. <https://doi.org/10.7150/thno.53105>